Bull. Mater. Sci. (2022) 45:251
https://doi.org/10.1007/s12034-022-02836-9

Effects of S/EB ratio on some properties of PLA/SEBS blends

İ EKIZ[1,2], M S CETIN[1,2], O TOPRAKCI[1,2] and H A KARAHAN TOPRAKCI[1,2,*]
[1]Department of Polymer Materials Engineering, 77200 Yalova, Turkey
[2]Institute of Graduate Studies, Yalova University, 77200 Yalova, Turkey
*Author for correspondence (aylin.toprakci@yalova.edu.tr)

MS received 8 April 2022; accepted 13 August 2022

Abstract. Poly(lactic acid) (PLA)/styrene-*b*-(ethylene-*co*-butylene)-*b*-styrene (SEBS) blends were prepared by using two different SEBS polymers with different styrene to ethylene–butylene (S/EB) ratio. Polymer blends were prepared by high shear solution mixing and solvent-casted samples were compression moulded. PLA/SEBS blends with the ratio of 25/75, 50/50 and 75/25 were prepared and their morphological, mechanical, structural and thermal properties were evaluated. Scanning electron microscopy analysis showed that S/EB ratio was important in terms of morphology of the phase separation. While at lower S content, phase separation was mostly in the form of cylindrical channels, and at higher S ratio, copolymer dispersed in PLA in the form of random spherical particles and cylindrical channels. Although incorporation of SEBS led to decrease in tensile strength and increase in strain at break for both copolymers, higher S ratio resulted in higher strength and modulus. Thermal stability of PLA showed almost similar properties by addition of copolymers, regardless of the copolymer morphology. Fourier transform infrared spectroscopy and differential scanning calorimetry analyses showed the characteristic behaviour of the polymers. Blends did not show noticeable shift for glass transition temperature (T_g) in terms of their SEBS component. However, T_{gPLA} shifted to lower values and double peaks that are useful for understanding the melting behaviour of the system, turned into a single peak.

Keywords. Poly(lactic acid); styrene-*b*-(ethylene-*co*-butylene)-*b*-styrene; polymeric blends; thermoplastic elastomer; block copolymer; phase separation.

1. Introduction

Poly(lactic acid) (PLA) is a rigid polymer with high elastic modulus and low tensile strain. In order to modify its morphological, thermal and mechanical properties, it can be blended with different polymers [1–3]. Styrene-*b*-(ethylene-*co*-butylene)-*b*-styrene (SEBS) is a styrene-based thermoplastic elastomer, and the most important feature of this polymer is that it acts both as an elastomer and as a thermoplastic. The studies about PLA/SEBS blends can be classified as: PLA/SEBS blends [4,5], PLA/maleated SEBS (SEBS-g-MAH) blends [6–10], PLA/SEBS multicomponent blends [5,10–12] and PLA-g-SEBS copolymers [13]. In these studies the blends were generally prepared by melt mixing [5,7,8,13–15]; SEBS or SEBS-g-MAH content was reported around 5–40 wt% [4,5,7,14–16], S/EB ratios were 29/71 [14,15], 30/70 [4], 30.5/69.5 [8], 34/66 [5].

In one of these studies, effects of PLA/SEBS content on mechanical and thermal properties were investigated. SEBS content was found significant in terms of mechanical, rheological and morphological properties [4]. Hashima *et al* [5] observed increase in thermal stability, impact strength and tensile strain, while decrease in tensile strength after SEBS addition [5]. In order to increase the compatibility between PLA and SEBS and compensate the decrease in tensile strength, PLA/SEBS-g-MAH blends were also investigated, but in some studies grafting degree (MAH/SEBS) or S/EB ratio were not given [9]. As reported by many authors, PLA/SEBS-g-MAH blends generally showed lower elastic modulus, tensile strength, and higher tensile strain and impact resistance compared to PLA [7,9,15,16]. In other study, SEBS and SEBS-g-MAH were compared and impact strength of PLA/SEBS-g-MAH blend was found higher compared to SEBS/PLA blends [8]. In another study, maleinized linseed oil (MLO) was used as a bio-compatibilizer for PLA/SEBS blends, in which PLA/SEBS/SEBS-g-MAH, PLA/SEBS/MLO, PLA/SEBS/SEBS-g-MA/MLO blends were prepared and their mechanical performance was compared. While PLA/SEBS/MLO showed better tensile strength compared to PLA/SEBS/SEBS-g-MAH, and PLA/SEBS/SEBS-g-MA/MLO showed the highest tensile strength [9]. In multicomponent PLA blends, SEBS and SEBS-g-MAH were generally used as a compatibilizer [11,17]. In order to increase the compatibility between two phases, PLA-g-SEBS copolymers were also used in the literature [13]. Based on this literature, SEBS content in PLA/SEBS blends was around 5–40 wt%, S/EB ratio was around 30/70 and blends were obtained by melt mixing. To

Published online: 17 December 2022

the extent of the recent literature, no study was found in the literature that investigated the block ratio effect of SEBS on the properties of solution mixed PLA/SEBS blends. As known, S/EB ratio directly effects the mechanical, rheological and thermal properties of the SEBS. Since S phase has higher glass transition temperature (T_g) than EB phase, SEBS matrixes with lower S content ($S \leq 20$) have relatively lower T_g, compared to SEBS with higher S content ($S > 20$) [18], and they have higher strain values at break [19] that is significant for fabrication of flexible and stretchable PLA films. In this study, to investigate the processing and blending performance with PLA, two different SEBS polymers with low S content (13/87, 19/81) were used for the first time in the literature. To maximize the physical interaction between PLA–SEBS and consequently blending efficiency, samples were prepared via solution casting with a high-shear planetary mixer. Planetary high shear mixers are systems with the ability of fast and homogeneous mixture preparation. More homogeneous phase dispersion can be obtained compared to traditional mechanical mixers in couple of minutes. After drying, casted films were compression moulded and characterized for their morphological, mechanical, structural and thermal properties.

2. Experimental

2.1 *Materials*

PLA and two different SEBS polymers were used. Melt flow index of PLA (MFI) was 8 g/10 min (210°C). The S/EB ratio and MFI value of SEBS1 (Kraton, G1657) were 13/87 and 8 g/10 min (200°C), respectively. The S/EB ratio and MFI value of SEBS2 (Kraton, G1643) were 19/81, MFI 75 g/10 min (200°C), respectively. Toluene and tetrahydrofuran were used as the solvents. The weight average-molecular weight (M_w) of SEBS1 and SEBS2 were 70 [20] and 139 kDa [21], respectively.

2.2 *Methods*

PLA/SEBS blends were prepared with the following wt%/wt% contents: 100/0, 75/25, 50/50, 25/75 and 100/0. Sample codes and contents are listed in table 1. Following this to increase the interaction between polymers, PLA and SEBS solutions were mixed by a high shear mixer (Kurabo Mazerustar KK 250) and casted into the Petri dishes (figure 1). After samples were dried for 24 h at 40°C and 4 h at 80°C under vacuum (Wisd, WOV-20), they were compression moulded between Teflon-coated plates at 190°C for 90 s and cooled down at 25°C for 120 s (figure 1).

Table 1. Sample codes and contents.

Sample codes	PLA (wt%)	SEBS1 (wt%)	SEBS2 (wt%)
PLA	100	—	
SEBS1	—	100	—
SEBS2	—	—	100
75/25 PLA/SEBS1	75	25	—
50/50 PLA/SEBS1	50	50	—
25/75 PLA/SEBS1	25	75	—
75/25 PLA/SEBS2	75	—	25
50/50 PLA/SEBS2	50	—	50
25/75 PLA/SEBS2	25	—	75

3. Characterization of the blends

3.1 *Morphological analysis*

Quanta 400F field-emission scanning electron microscope (FESEM) at 20 kV was used for cross-sectional morphology analysis of the samples. To observe the phase behaviour of the polymers, samples were cryo-fractured in liquid nitrogen and sputter-coated (Au/Pd alloy, 3–6 nm) before the analysis.

3.2 *Mechanical characterization*

Devotrans, DVT GPU/RD mechanical testing system was used for the determination of stress–strain behaviour of the samples. The stress–strain graphs were given as engineering stress and strain. Asimeto thickness metre was used before the test. The test speed was set to 50 mm min^{-1}, and specimens with the dimensions of 5×20 mm (width×length) were cut by a blade, four specimens were tested and average values and standard deviations were calculated.

3.3 *Fourier transform infrared spectroscopy*

Perkin Elmer, Spectrum 100 system was used for Fourier transform infrared (FTIR) analysis (ATR mode). Spectra were recorded between 650 and 4000 cm^{-1} in the transmittance mode (spectral resolution: 4 cm^{-1}, scan rate: 4 scans).

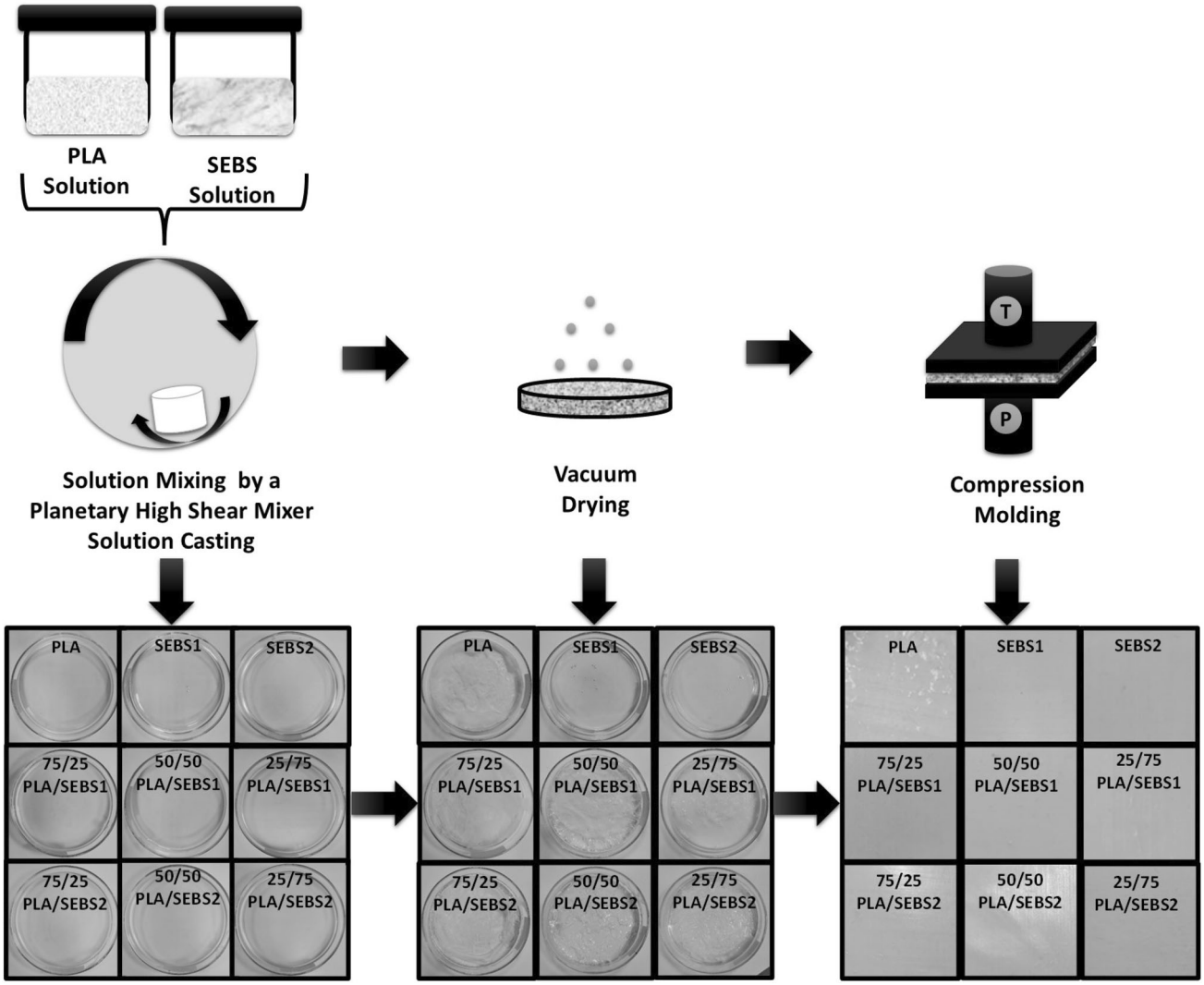

Figure 1. Preparation steps and digital images of the samples after each step.

3.4 *Thermogravimetric analysis*

Seiko, TG/DTA 6300 was used for thermogravimetric analysis (TGA). Tests were carried out between 25 and 610°C under the nitrogen atmosphere. Gas flow rate and temperature increase rate were 200 ml min^{-1} and 10 C min^{-1}, respectively.

3.5 *Differential scanning calorimetry*

Perkin Elmer Diamond testing system was used for the differential scanning calorimetry (DSC) analysis of the samples. The heating/cooling rate was 10°C min^{-1} from –90 to 200°C under N_2 atmosphere.

4. Results and discussion

4.1 *Morphological analysis*

Blend morphology is basically related with the scale, size, geometry, shape, spatial distribution of the phase separation. As known, blend morphology is directly affected by the polymer type and ratio of the components. Generally, at low concentrations, dispersed phase is found in spherical geometry, while at higher concentrations cylindrical channels, fibrious or sheet-like geometry can be observed [22]. In order to observe the difference between SEBS1 and SEBS2 and observe the maximum interaction between PLA and SEBS, 50/50 blend ratio was chosen for the SEM analysis.

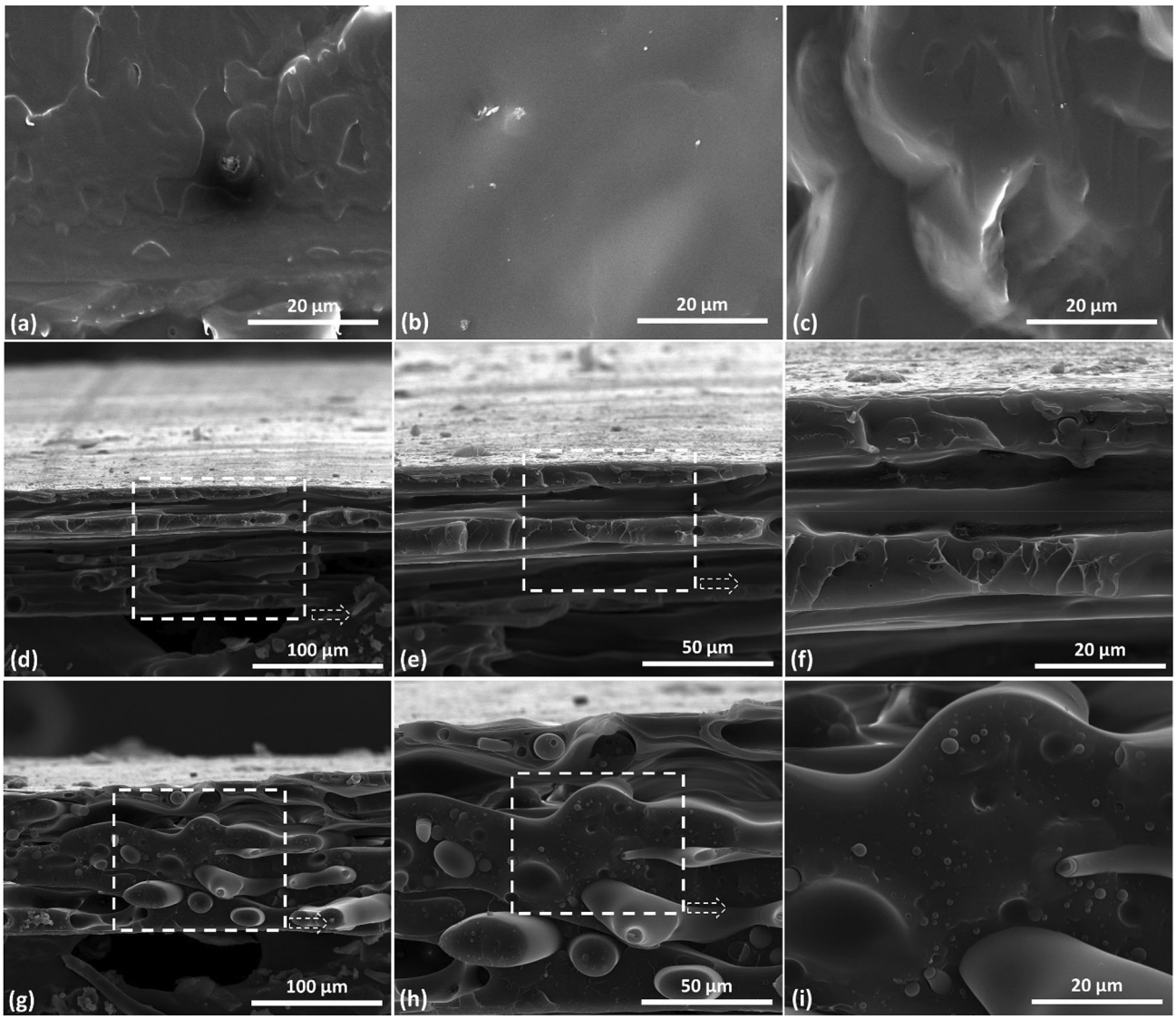

Figure 2. SEM images of (**a**) PLA, (**b**) SEBS1, (**c**) SEBS2, (**d–f**) 50/50 PLA/SEBS1 and (**g–i**) 50/50 PLA/SEBS2.

Morphology of the specimens were analysed from the cryo-fractured cross-sections, those can be seen from figure 2. PLA, SEBS1 and SEBS2, can be seen from figure 2a–c. PLA/SEBS1 and PLA/SEBS2 can be seen from figure 2d–f and g–i, respectively. To analyse phase distribution and phase interphase, SEM images were taken at different magnifications. As seen from figure 2d–f, PLA was the continuous phase and SEBS1 dispersed in PLA in the form of cylindrical channels. Since SEBS1 was removed during cryo-fracturing process, only channels could be seen. Although PLA was the continuous phase for SEBS2 blend, (figure 2d–f), blend morphology was different compared to first blend. Both random spherical particles and cylindrical channels were observed, which were probably caused by the S/EB ratio of the polymers. SEBS1 and SEBS2 had the S/EB ratio as 13/87 and 19/81, respectively. Higher styrene ratio and high MFI value of SEBS2 assumed to cause higher level of interaction, and PLA/SEBS2 blend showed better mixing.

4.2 *Mechanical analysis*

Stress–strain curves of PLA/SEBS1 and PLA/SEBS2 sets can be seen from figure 3a and b. Tensile strength, elastic modulus of the samples and tensile strain values are summarized in figure 3c and d, respectively (engineering stress and strain values are given). Average tensile strength, tensile strain and elastic modulus values of the samples can be seen from table 2. PLA showed typical stress–strain behaviour with 45.35 MPa tensile strength and 3% tensile strain. SEBS1 and SEBS2 had tensile strength as 7.5 and 9.7 MPa, respectively. Since SEBS2 had higher S ratio (S/EB 19/81), and high molecular weight it showed higher resistance to break. On the other hand, SEBS2 had lower tensile strain because of lower EB ratio and lower molecular weight. Tensile strain values of SEBS1 and SEBS2 were determined as 832 and 819%, respectively. The elastic modulus of PLA, SEBS1

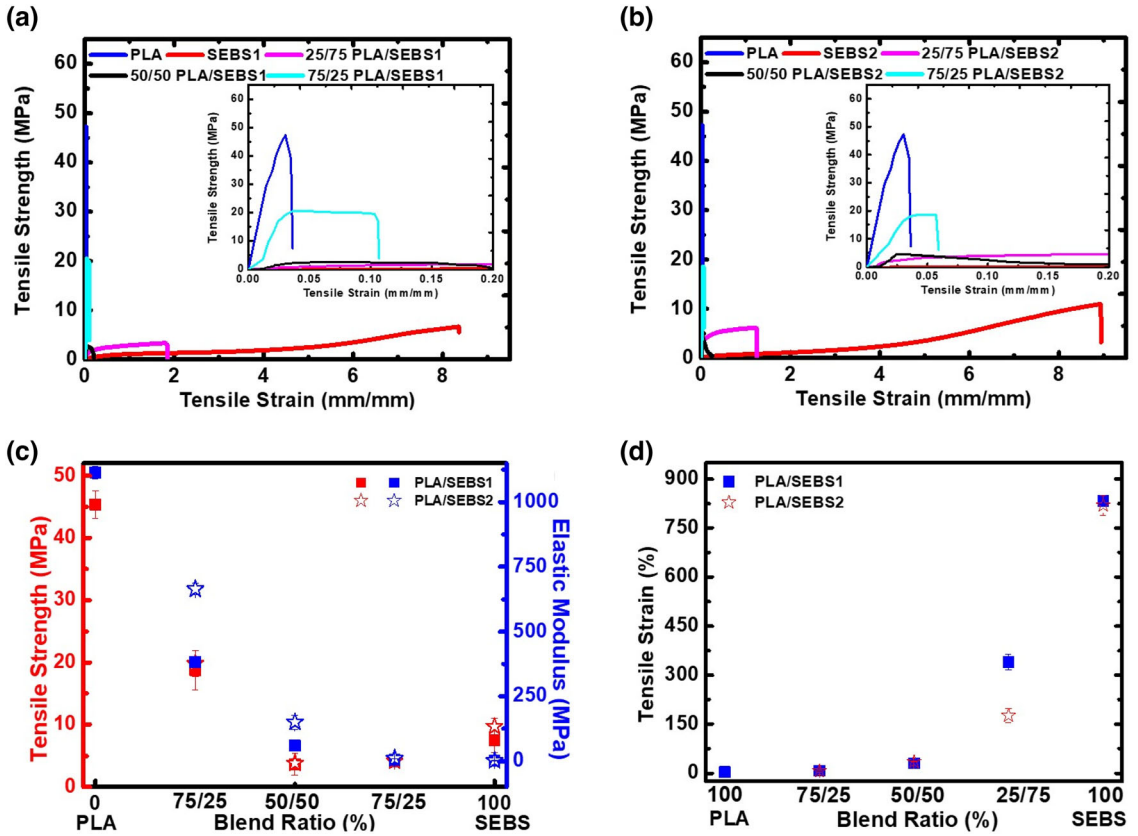

Figure 3. Stress–strain curves of neat and blend films: (**a**) PLA/SEBS1 set and (**b**) PLA/SEBS2 set. (**c**) Tensile strength and elastic modulus of the samples as a function of blend content. (**d**) Tensile strain values of the samples as a function of blend content.

Table 2. Mechanical properties of PLA, SEBS1, SEBS2 and PLA/SEBS blends.

Sample codes	Tensile strength (MPa)	SD	Tensile strain (%)	Elastic modulus (MPa)
PLA	45.4	2.25	3.8	1113.9
SEBS1	7.5	2.06	832.7	1.9
SEBS2	9.7	1.33	819.4	2.2
75/25 PLA/SEBS1	18.8	3.15	7.3	382.2
50/50 PLA/SEBS1	3.6	1.70	30.3	58.6
25/75 PLA/SEBS1	4.0	0.76	339.5	4.8
75/25 PLA/SEBS2	19.8	2.16	6.6	663.7
50/50 PLA/SEBS2	3.8	0.76	35.5	148.9
25/75 PLA/SEBS2	4.2	0.5	175.9	10

and SEBS2 were calculated as 1113, 1.9 and 2.2 MPa, respectively. By incorporation of SEBS into PLA, the narrow stress–strain peak became wider and both tensile strength and tensile strain values were found in between PLA and SEBS, which is an indication of good blending. Figure 3 clearly shows that by increasing the SEBS content in PLA/SEBS blends, tensile strength values dropped and strain at break increased gradually. 75/25, 50/50 and 25/75 PLA/SEBS1 blends showed tensile strength values as 18.8, 3.6 and 4.0 MPa, respectively. 75/25, 50/50 and 25/75 PLA/SEBS2 blends showed tensile strength values as 19.8, 3.8 and 4.2 MPa, respectively. These outcomes were also supported by SEM images. As given in figure 2, the dispersion and mixing performance of SEBS2 was better compared to SEBS1 that also led to higher tensile strength. For both sets, 25/75 PLA/SEBS blends showed slightly higher values than 50/50 blends. In 25/75 blend content, SEBS was in the continuous phase and at 25 wt% PLA concentration, level of phase separation was probably lower compared to 50 wt%. 75/25,

50/50, and 25/75 PLA/SEBS1 and 75/25, 50/50, and 25/75 PLA/SEBS2 blends had tensile strain values 226 7.3, 30.3, 339.5% and 6.6, 35.5, 175.9%, respectively. Since SEBS1 had higher EB ratio, strain values were generally higher compared to SEBS2 blends. Parallel with these results, elastic modulus of the blends gradually dropped by increasing the SEBS ratio. PLA/SEBS2 blends showed higher elastic modulus values that was probably caused by higher styrene content of SEBS2 and higher molecular interaction between PLA and SEBS.

4.3 *FTIR spectroscopy*

The characteristic peaks that belong to IR spectrum of PLA can be seen from table 3. The peaks at 2996 and 2946 cm^{-1} were assigned to –C–H stretching. The peak at 1747 cm^{-1} was related to –C=O stretching vibrations of carbonyl group. Deformation vibration of $–CH_3$ bonds was observed at 1451 cm^{-1}. The peaks at 1382, 1365 and 1360 cm^{-1} represented –CH– deformation, C–H stretching methyl groups and bending vibration of $–CH_3$ bonds. The peaks at 1213 and 1181 cm^{-1} were due to C–C stretches and C–O–C symmetric stretching vibrations in ester groups of PLA. The peaks at 1127, 1080 and 1043 cm^{-1} were related to C–O bond deformation vibrations in CH–O groups in PLA. The peaks at 957, 869, 755 cm^{-1} were assigned to C–C and C–H-bond stretches [23–28].

As expected, almost same peaks were observed for SEBS1 and SEBS2 with slight differences. The peaks around 2959, 2920 and 2851 cm^{-1} were assigned to C–H stretching [29–32]. Since SEBS1 has higher EB ratio, the peak intensity was higher compared to SEBS2. The peak around 1600 cm^{-1} was related with skeleton deformation vibration of aromatic ring moieties found in benzene ring. Although these peaks were observed for SEBS1 and SEBS2; SEBS2 showed slightly higher intensity probably caused by higher S ratio. The peaks around 1460 and 1380 cm^{-1} were due to symmetric $–CH_3$ bending and vibration of –CH on the methyl groups. The peak around 1028 and 759 cm^{-1} were assigned to C–H in-plane-deformation bending of aromatic ring [30,33], and styrenic –CH bending [34,35], respectively. The peak around 698 cm^{-1} was due to bending vibrations of styrene. As expected, SEBS2 showed higher intensity because of its higher S ratio.

The peaks around 2996–2946 cm^{-1} observed for PLA and peaks around 2959–2851 cm^{-1} observed for SEBS were also observed for PLA/SEBS blend in the form of a wider peak with lower intensity between 3000 and 2825 cm^{-1} in between PLA and SEBS. The carbonyl peak of PLA at 1747 cm^{-1} was also observed for PLA/SEBS1 at 1748 cm^{-1} and at 1747 cm^{-1} at for PLA/SEBS2. Since PLA and SEBS showed peaks between 1460 and 1350 cm^{-1}, as given in figure 4, PLA/SEBS blend also showed peaks around similar region. Between 1250 and 750 cm^{-1}, SEBS did not show any significant peak intensity, while in this range PLA/SEBS blend showed the same peaks observed for PLA. Similar with that, the peak observed for SEBS at 758 cm^{-1} was also observed for PLA/SEBS blends. All these can be given as an indication of good mixing.

4.4 *Thermal gravimetric analysis*

TGA analysis of the samples between 25 and 610°C can be seen from figure 5a and table 4. The thermal

Table 3. Characteristic IR peaks observed for PLA and SEBS.

Polymer	Band (cm^{-1})	Assignment	Reference
PLA	2996, 2946	–C–H stretching	
	1747	–C=O stretching of carbonyl group	[36]
	1451	$–CH_3$ deformation	[36]
	1382	–CH– deformation	
	1365	–C–H stretching methyl group	
	1360	bending of $–CH_3$	
	1213	C–C stretches	
	1181	C–O–C symmetric stretching	
	1127	–C–O stretching	[36]
	1080,1043	–C–O-bond deformation vibrations	[24,25,36]
	957	–C–C stretch	[23,25]
	869, 755	–C–H-bond stretches	[24,25]
SEBS	2959, 2920, 2851	$–CH_2–$ asymmetric, $–CH_2–$ stretching vibrations	[37]
	1600	Deformation vibration of aromatic rings	[38]
			[38]
	1460, 1380	$–CH_3$ bending and vibration of –CH of methyl groups	[29,37,39]
	1028, 758	Aromatic sp^2 –CH bending	[39]
	698	Bending vibrations of styrene	[34]

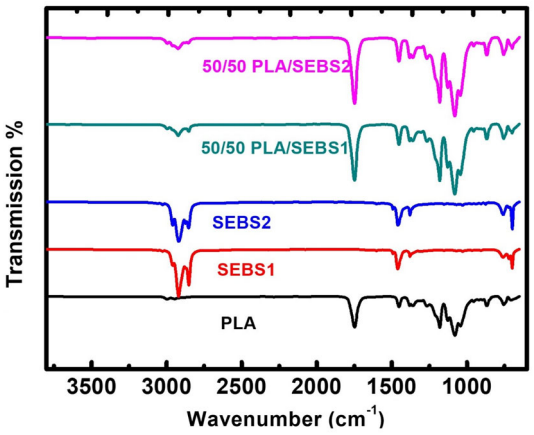

Figure 4. FTIR spectrum of the specimens.

degradation profile of PLA, SEBS1 and SEBS2 took place in one-step as previously reported in the literature [8,40,41]. T_{max} values were determined as 366, 453 and 443°C for PLA, SEBS1 and SEBS2, respectively. As evident from these results, the thermal stability can be given as PLA<SEBS2<SEBS1; in other words, both SEBS showed higher thermal stability compared to PLA. Regardless of the SEBS type, blends showed two-step degradation profile. The first degradation step was related to PLA degradation and the second step started after PLA decomposition and belonged to SEBS. As given in figure 5a, T_{max} values related with the two-step degradation profile were determined as 360/456°C for PLA/SEBS1 and 358/454°C for PLA/SEBS2 phases. The T_{max} values of PLA phase in the sample were 366, 360 and 358 for neat PLA, PLA/SEBS1 and PLA/SEBS2, respectively. Although the difference was not drastic, PLA showed lower T_{max} value in the blend form that was probably caused by increased surface area as given in SEM analysis. The T_{max} values of SEBS1 phase for neat SEBS1 and PLA/SEBS1 were determined as 453 and 456°C, respectively. The T_{max} values of SEBS2 phase for neat SEBS2 and PLA/SEBS2 were determined as 443 and 454°C, respectively. Although the difference was not huge, residuals of decomposed PLA might be the reason for that shift.

Figure 5b gives $T_{10\%}$, $T_{50\%}$ and $T_{70\%}$ values of the samples. While $T_{10\%}$ and $T_{50\%}$ values of the blends were close to PLA, $T_{70\%}$ values shifted to SEBS1 and SEBS2. Since samples composed of 50/50 PLA/SEBS, after PLA completely decomposed, residual part was dominantly SEBS and thermal degradation behaviour was almost same as SEBS1 and SEBS2. That is an indication of good and homogeneous mixing of the samples. In addition to that, thermal stability of SEBS1 was slightly higher than SEBS2, PLA/SEBS1 showed a more flat and broad plateau-type degradation profile in the second step compared to PLA/SEBS2 blend.

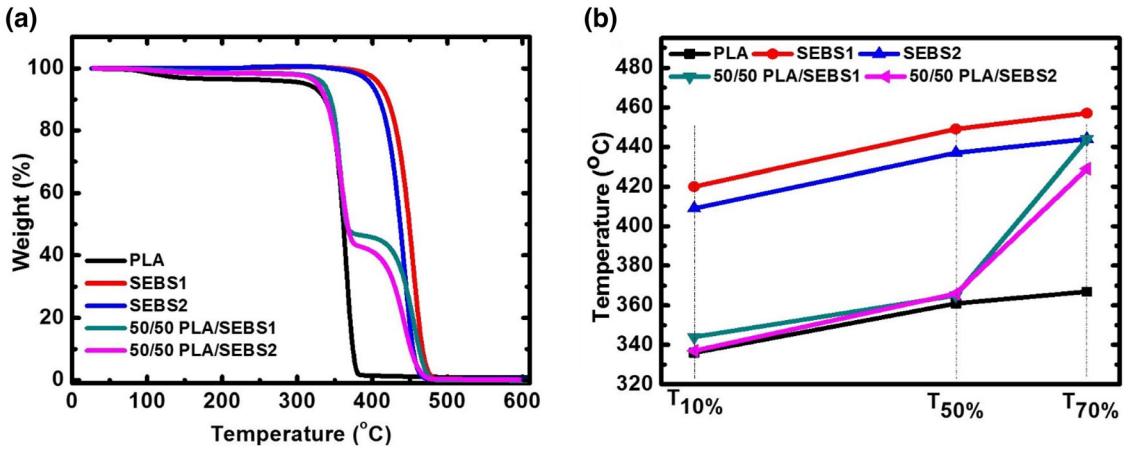

Figure 5. (**a**) TGA curves between 25 and 610°C, and (**b**) $T_{10\%}$, $T_{50\%}$, $T_{70\%}$ values of the specimens.

Table 4. Thermal degradation behaviour of the specimens.

Sample codes	$T_{max\ degradation}$ (°C)	$T_{10\%}$ (°C)	$T_{50\%}$ (°C)	$T_{70\%}$ (°C)	Ash wt% @ 600°C
PLA	366	336	361	367	0.8
SEBS1	453	420	449	457	0.17
SEBS2	443	409	437	444	0.3
50/50 PLA/SEBS1	360/456	344	365	444	0.14
50/50 PLA/SEBS2	358/454	337	366	429	0.04

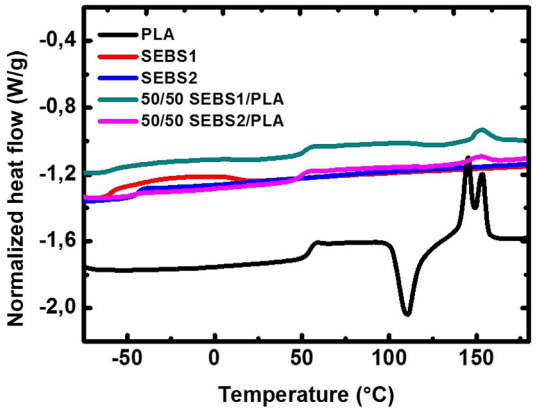

Figure 6. DSC thermograms of the specimens between –75 and 180°C.

4.5 *Differential scanning calorimetry*

Thermal properties of PLA, SEBS1, SEBS2, and 50/50 PLA/SEBS1 and 50/50 PLA/SEBS2 blends were determined by DSC (second heating run) and given in figure 6. Since PLA has a semi-crystalline morphology, glass transition temperature (T_g), cold crystallization temperature (T_c) and melting temperature (T_m) were observed. T_g and T_c were around 55 and 110°C, respectively. Two melting temperatures as T_{m1} and T_{m2} were determined around 145 and 153°C, respectively. SEBS1 and SEBS2 showed T_g values of –61 and –45°C, respectively. That difference was assumed to be caused by higher EB ratio of SEBS1 that led to higher chain mobility and free volume [19,42].

The incorporation of SEBS into PLA led to some changes in thermal properties. Cold crystallization peak of PLA almost disappeared for both blends. PLA/SEBS1 showed two T_g values around –61 and 51°C for SEBS1 and PLA phases of the blend. PLA/SEBS2 showed T_g values of –45 and 50°C for SEBS2 and PLA phases of the blend. While both blends did not show noticeable shift for T_g in terms of their SEBS component, T_g observed for PLA shifted to lower values because of increase in segmental motion of PLA macromolecules caused by elastic nature of SEBS1 and SEBS2 with higher chain mobility and free volume. For both blends, unlike neat PLA, only one peak was observed as T_m of PLA and determined around 152–153°C, which was an indication of one type of crystal formation [43,44].

5. Conclusions

In this study, PLA/SEBS blends were prepared and characterized. The purpose of the study was to fabricate and characterize PLA/SEBS blends with two matrixes that have different copolymer morphology based on S/EB ratio. Blends were prepared by solution casting and compression moulding. Morphological, mechanical, structural and thermal properties of the blends were analysed. The following conclusions can be given based on the outcomes of the study: SEM analysis showed that at lower S content, phase separation morphology of SEBS1 was in the form of cylindrical channels. However, at higher S ratio, SEBS2 was observed as the dispersed phase in PLA in the form of random spherical particles and cylindrical channels. Higher styrene ratio and MFI value led to higher level of interaction, and PLA/SEBS2 blend showed better mixing. Incorporation of SEBS led to decrease in tensile strength and increase in strain at break. PLA/SEBS2 blends showed higher tensile strength and elastic modulus and lower tensile strain. Thermal degradation behaviour of the blends showed two-step degradation profile, in which first step belonged to PLA and second step belonged to SEBS and no drastic difference was observed between the blends. Specimens showed characteristic blend behaviour in the DSC analysis. Although significant shift was not observed, T_{gSEBS}, T_{gPLA} shifted to lower values and double peaks related with T_m turned into a single peak representing the melting behaviour of the system.

Acknowledgement

This project was funded by the Yalova University, BAP (Scientific Research Project) Project No: 2021/YL/0013, 'Preparation and Characterization of Poly(lactic acid) Blends'.

References

[1] Saeed U, Nawaz M A and Al-Turaif H A 2018 *J. Compos. Mater.* **52** 19
[2] Hazer S and Aytac A 2021 *J. Compos. Mater.* **55** 8
[3] Chow W S, Leu Y Y and Ishak Z M 2014 *J. Compos. Mater.* **48** 2
[4] Lima J C C, Araújo E A G, Agrawal P and Mélo T J A 2019 *Macromol. Symp.* **383** 1
[5] Hashima K, Nishitsuji S and Inoue T 2010 *Polymer (Guildf)* **51** 17
[6] Nehra R, Maiti S N and Jacob J 2018 *Polym. Adv. Technol.* **29** 1
[7] Lu Y, Wang C, Yu J and Lu S 2018 *IOP Conf. Ser. Mater. Sci. Eng.* **394** 2
[8] Sangeetha V H, Varghese T O and Nayak S K 2016 *Polym. Eng. Sci.* **56** 6
[9] Tejada-Oliveros R, Balart R, Ivorra-Martinez J, Gomez-Caturla J, Montanes N and Quiles-Carrillo L 2021 *Molecules* **26** 1
[10] Jiang J, Su L, Zhang K and Wu G 2013 *J. Appl. Polym. Sci.* **128** 6
[11] Arvidson S A, Roskov K E, Patel J J, Spontak R J, Khan S A and Gorga R E 2012 *Macromolecules* **45** 2
[12] Park D H, Kim M S, Yang J H, Lee D J, Kim K N, Hong B K *et al* 2011 *Macromol. Res.* **19** 2

[13] Qi R, Luo M and Huang M 2011 *J. Appl. Polym. Sci.* **120** 5
[14] Tsou C H, Kao B J, Yang M C, Suen M C, Lee Y H, Chen J C *et al* 2015 *Biomed. Mater. Eng.* **26** 147
[15] Nehra R, Maiti S N and Jacob J 2018 *J. Appl. Polym. Sci.* **135** 1
[16] Sangeetha V H, Varghese T O and Nayak S K 2019 *Iran. Polym. J. (English Ed.)* **28** 8
[17] Yoo T W, Yoon H G, Choi S J, Kim M S, Kim Y H and Kim W N 2010 *Macromol. Res.* **18** 6
[18] Arevalillo A, Muñoz M E, Calafell I, Santamaría A, Fraga L and Barrio J A 2012 *Polym. Test.* **31** 7
[19] Cetin M S and Karahan Toprakci H A 2021 *Compos. Part B Eng.* **224** 109199
[20] Daniel C, Hamley I W and Mortensen K 2000 *Polymer (Guildf)* **41** 26
[21] Zhu S, So J H, Mays R, Desai S, Barnes W R, Pourdeyhimi B *et al* 2013 *Adv. Funct. Mater.* **23** 18
[22] Utracki L A and Wilkie C A 2014 (eds) *Polymer blends handbook* (Netherlands: Springer)
[23] Lee H W, Insyani R, Prasetyo D, Prajitno H and Sitompul J 2015 *J. Eng. Technol. Sci.* **47** 4
[24] Muller J, González-Martínez C and Chiralt A 2017 *Eur. Polym. J.* **95** 56
[25] Liu Y, Liang X, Wang S, Qin W and Zhang Q 2018 *Polymers (Basel)* **10** 5
[26] Pop M A, Croitoru C, Bedő T, Geaman V, Radomir I, Coşniţa M *et al* 2019 *J. Appl. Polym. Sci.* **136** 17
[27] Bolskis E, Adomavičiute E, Griškonis E and Norvydas V 2020 *Materials (Basel)* **13** 17
[28] Harmaen A S, Khalina A, Faizal A R and Jawaid M 2013 *Polym. Plast. Technol. Eng.* **52** 4
[29] Dong W, Wang X, Jiang Z, Tian B, Liu Y, Yang J *et al* 2019 *Polymers (Basel)* **11** 6
[30] Ganguly A, Bhowmick A K and Li Y 2008 *Macromolecules* **41** 16
[31] Mistry M K, Choudhury N R, Dutta N K and Knott R 2010 *J. Memb. Sci.* **351** 1
[32] Vargas M A, López N N, Cruz M J, Calderas F and Manero O 2009 *Rubber Chem. Technol.* **82** 2
[33] Asandulesa M, George R, Topala I, Pohoata V, Dobromir M and Dumitrascu N 2013 *Open Plasma Phys. J.* **6** 1
[34] Kim J, Keun, Kim C, Hyeon, Park M and Hwan 2016 *Bull. Korean Chem. Soc.* **37** 6
[35] Garcia-Garcia D, Crespo-Amorós J E, Parres F and Samper M D 2020 *Polymers (Basel)* **12** 4
[36] Liu S, Wu G, Chen X, Zhang X, Yu J, Liu M *et al* 2019 *Polymers (Basel)* **11** 6
[37] Bhadusha N and Ananthabaskaran T 2011 *J. Chem.* **8** 4
[38] Luisa L, Esteves B and Martins J M 2012 *5th Int. Conf. Environ. Compat. For. Prod. (PROCEEDINGS ECOWOODV12)*
[39] Cetin M S, Toprakci O, Taskin O S, Aksu A and Toprakci H A K 2022 *J. Elastomers Plast.* **54** 1
[40] Zhang J B, Zhang H, Jin F L and Park S J 2020 *Bull. Mater. Sci.* **43** 1
[41] Cui X, Jiang Y, Xu Z, Xi M, Jiang Y, Song P *et al* 2021 *Compos. Part B Eng.* **211** 108641
[42] Costa P, Silva J, Ansón-Casaos A, Martinez M T, Abad M J, Viana J *et al* 2014 *Compos. Part B Eng.* **61** 136
[43] Teamsinsungvon A, Ruksakulpiwat Y and Jarukumjorn K 2013 *Polym. Plast. Technol. Eng.* **52** 13
[44] Zhang J, Yan D X, Xu J Z, Huang H D, Lei J and Li Z M 2012 *AIP Adv.* **2** 4